2016 IEEE International Conference on Manipulation, Manufacturing and Measurement on the Nanoscale (3M-NANO)
18-22 July, Chongqing

Back Propagation Neural Networks Based Hysteresis Modeling and Compensation for a Piezoelectric Scanner

Yinan Wu[1,2], Yongchun Fang[1,2], Xiao Ren[1,2], and Han Lu[1,2]
1. Institute of Robotics and Automatic Information System, Nankai University, Tianjin, 300350, China
2. Tianjin Key Laboratory of Intelligent Robotics, Tianjin, 300350, China

***Abstract*—As the actuator of a common atomic force microscopy (AFM), a piezoelectric scanner has many advantages than other actuators, such as high precision of displacements on the nanoscale, high efficiency of electromechanical coupling, rapid response and so on. However, hysteresis nonlinearity of a piezoelectric scanner affects the positioning of the scanner and image quality of an AFM system. In this paper, a modeling method based on Back Propagation Neural Networks (BPNN) is proposed to compensate for hysteresis behavior. In particular, considering memory characteristics and frequency dependence of the hysteresis effect, firstly, we utilize a two hidden layers BPNN consisting of an input layer including the frequency and a section of the input voltage, two hidden layers, and an output layer to model for hysteresis. Subsequently, a method based on cubic spline interpolation is proposed to compensate for hysteresis behavior. Experiment results demonstrate the high precision of the obtained hysteresis model and the good performance of the proposed compensation method.**

***Index Terms*—Atomic Force Microscopy, Hysteresis, Back Propagation Neural Networks**

I. Introduction

Because of its significant advantages in many aspects, an atomic force microscope (AFM) has been applied in lots of fields, such as nanomanipulation, nanotechnology and biotechnology [1]. An AFM utilizes a tiny probe to scan detected samples to obtain the image, the basic principle is to keep the force between the probe tip and the atoms of samples' surface remain unchanged [2]. In this way, an AFM can acquire the image resolution on the nanoscale without limiting the electrical conductivity of samples [3]. Moreover, the probe can scan samples both in gaseous and liquid environment, which makes the AFM available in some liquid biological experiments [4]. In a word, an AFM has more advantages than traditional optical microscopes and it will be a irreplaceable tool in more and more fields [5].

For a common AFM system, a three dimensional piezoelectric scanner is usually employed as an actuator to generate displacements in nanometer level, including x, y lateral periodic trajectory for scanning process and the constant force control in z-direction [6]. Compared with other actuators, the piezoelectric scanner has many inimitable superiorities, such as high precision of displacements on the nanoscale, high efficiency of electromechanical coupling, rapid response and so on [7]. However, due to the influence of ferroelectric effect, the hysteresis nonlinearity of the piezoelectric scanner is caused. And the hysteresis nonlinearity becomes more pronounced with the increase of the frequency of the input driving voltage, which affects the positioning of the piezoelectric scanner and the image quality of the AFM system [8].

After noticing the impact of the hysteresis on the performance of the AFM system, many researchers have attempted all kinds of methods to address this problem. For example, H. Tang *et al.* proposed an image-based method by using polar coordinate to model the piezoelectric scanner utilized in AFM, which could effectively avoid the troubles of data acquisition in AFM system [9]. Besides, in [10], K. K. Leang *et al.* presented the design of a high-gain feedback controller to account for hysteresis effects without modeling the complicated nonlinear behavior and the feedforward input improved the performance of the feedback controller significantly. In addition, Y. Zhang *et al.* proposed an image-based method to model the hysteresis characteristic of the AFM piezo-scanner. Based on the obtained model, a numerical recursive inversion-based compensator was designed to largely eliminate the effect of hysteresis [11]. In [12], D. Habineza *et al.* presented a new multivariable hysteresis Bouc-Wen model model and a compensator based on the combination of the inverse multiplicative structure with the mode to compensate for the hysteresis in a 3-DoF piezoelectric tube actuator. The experimental results demonstrated the proposed method could linearize the hysteresis in the direct transfers and to minimize the hysteresis of the cross-couplings.

Considering of the complexity of the hysteresis nonlinearity, it is difficult to utilize a simple mathematical model to describe the hysteresis effect. However, it is encouraging that Back Propagation Neural Networks (BPNN) has been demonstrated the feasibility of capturing nonlinear interactions between various parameters in complex systems [13]. Therefore, in this paper, we make effort to apply a two hidden layers BPNN consisting of an input layer, two hidden layers, and an output layer to model for the hysteresis. To be specific, firstly, considering of the memory characteristics and the frequency dependence of the hysteresis effect, we set the frequency of input voltage and a section of the input voltage including the voltage values of the current moment and the previous several moments as the input nodes of the BPNN. After continually iterative training, the final weights and thresholds which make the network error sum of squares minimum are determined. In

this way, the hysteresis modeling related to the frequency is completed. Then we propose a method based on cubic spline interpolation to compensate for the hysteresis behavior and improve the performance of the AFM system.

The rest of the paper is organized as follows. In Section 2, we introduce the hysteresis effect of the piezoelectric scanner in detail and analyze the main characteristics of the hysteresis. In Section 3, we utilize a two hidden layers BPNN to model for the hysteresis behavior and propose a method based on cubic spline interpolation to realize the hysteresis compensation to improve the AFM performance. Then, Section 4 presents the experiment results to demonstrate the performance of the proposed modeling and compensation method. Finally, the conclusions of this paper are made in the Section 5.

II. Analysis of the Hysteresis Effect

For a traditional AFM system, under normal circumstances, a set of triangular/sine wave voltage is set as the input voltage of the piezoelectric scanner in x-direction to actuate the back and forth movement. Because of the hysteresis nonlinearity of the piezoelectric scanner, the relationship between the output displacement and the input voltage is nonlinear [14]. When the input voltage alternately increases and decreases, a typical mark of hysteresis is that the output forms a loop as shown in Fig. 1, the red line and the blue line respectively represent the forward and backward scanning, the black dotted line represents the desired displacement. On account of the hysteresis effect, the hysteresis loop is generated which makes the deviation between the output displacement and the desired displacement. So the obtained height information of the scanning points is not matching to the corresponding points, which leads to the distortion of the image. In addition, the hysteresis effect has a memory characteristic, to be specific, the output displacement is not only determined by the current input voltage but also related to the history features and the change of the input voltage [15]. This characteristic leads to the different of the output displacement between the forward and backward scanning.

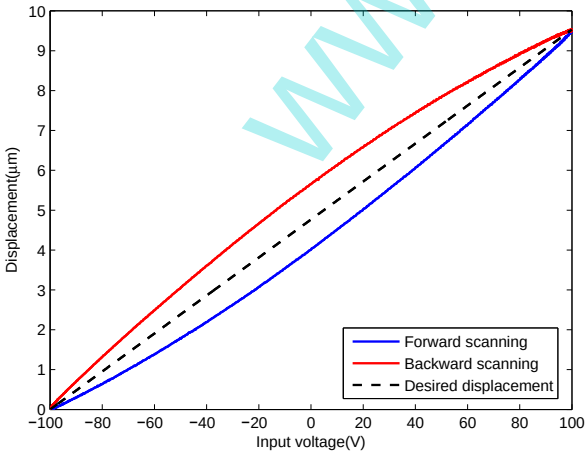

Fig. 1: The hysteresis effect of the piezoelectric scanner with frequency $5Hz$

The degree of hysteresis nonlinearity depends on many factors, among which the frequency of input voltage is an all-important factor. As shown in Fig. 2, the black, blue and red line respectively represent the hysteresis loop of the piezoelectric scanner with $1Hz$, $30Hz$ and $60Hz$. With increasing the frequency of the input driving voltage, the hysteresis loop becomes wider which means the hysteresis effect is more pronounced. In the meantime, the displacement of the scanner decreases with the increase of the frequency. When an AFM is operated with high frequency, the hysteresis effect could result in severely distorted tip displacements which leads to the poor image quality and the low positioning accuracy. Therefore, the hysteresis effect reduces the bandwidth and performance of the AFM system [16].

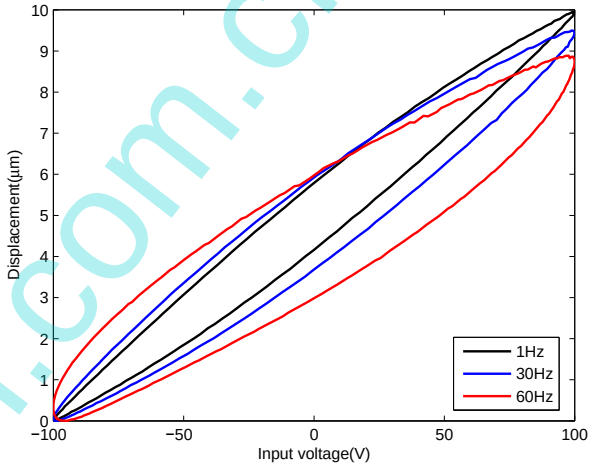

Fig. 2: The hysteresis effect of the piezoelectric scanner with different frequency of the input voltage

III. Hysteresis Modeling and Compensation

A. Hysteresis Modeling Based on Back Propagation Neural Networks

Noticing this drawback of the traditional AFM system, firstly, we utilize a BPNN to build the hysteresis model of piezoelectric scanner in x-direction. A BPNN is a neural network which utilizes the back-propagation learning algorithm to adjust weights and thresholds continually [17]. In a BPNN, the mathematical relationships between the various variables are not specified. Instead, they learn from the examples fed to them [18]. In addition, they can generalize correct responses that only broadly resemble the data in the learning phase. The BPNN with a single hidden layer has been shown to be capable of providing an accurate approximation of any continuous function provided there are sufficient hidden neurons [19].

In this research, considering of the memory characteristics of the hysteresis effect [20], we choose a section of the input voltage rather than the current single voltage as an input of a BPNN. Furthermore, because the hysteresis effect is related to the frequency of the input voltage, so the frequency is also input to a BPNN. After repeated experiments, we utilize a

two hidden layers BPNN consisting of an input layer, two hidden layers, and an output layer to model for the hysteresis. As shown in Fig. 3, the input layer is composed of ten nodes, of which x_1 to x_9 represent a section of the input voltage including the voltage values of the current moment and the previous eight moments, x_{10} represents the frequency of the input voltage. h_j and $\hat{h}_k$ respectively represent the hidden nodes of the first and second hidden layer, wherein $j \in \{1, 2 \ldots, 12\}, k \in \{1, 2 \ldots, 6\}$. y is the output node which represents the output displacement. $\omega_{ij}, \tilde{\omega}_{jk}$ and $\hat{\omega}_k$ are the weights between the adjacent layers.

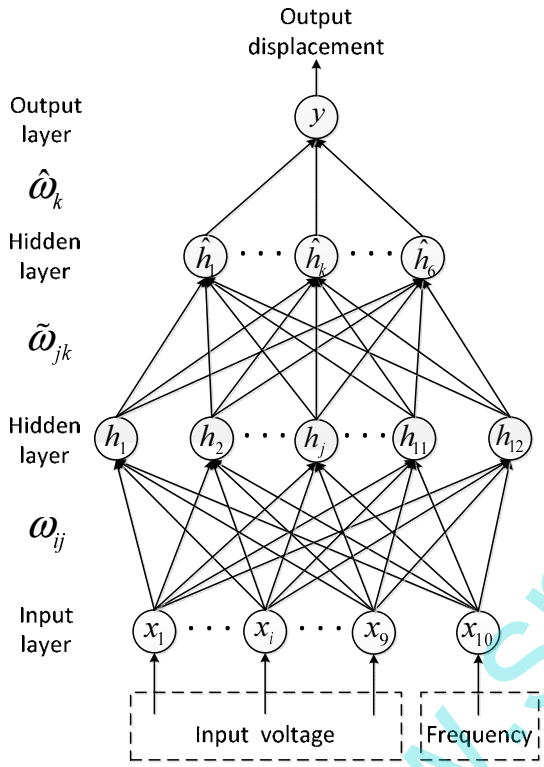

Fig. 3: The structure diagram of the adoptive BPNN

Then we can get the relationship between the input layer and the first hidden layer as follows:

$$h_j = f[\sum_{i=1}^{10}(x_i \omega_{ij}) + \alpha_j] \tag{1}$$

where α_j represent the threshold corresponding to each node of the first hidden layer, f represents the transfer function $tansig$ of the form

$$tansig(t) = \frac{2}{1 + e^{-2t}} - 1 \tag{2}$$

where t represents independent variable.

Similarly, the nodes of the second hidden layer can be calculated as follows:

$$\hat{h}_k = f[\sum_{j=1}^{12}(h_j \tilde{\omega}_{jk}) + \beta_k] \tag{3}$$

where β_k represent the threshold corresponding to each node of the second hidden layer.

Then the output displacement is calculated as follows:

$$y = f[\sum_{k=1}^{6}(\hat{h}_k \hat{\omega}_k) + \gamma] \tag{4}$$

where γ represents the threshold of the output node.

By utilizing the formula (1)-(4), the hysteresis model related to the frequency is obtained. Then we set formula (5) as the input voltage to obtain the weights and thresholds.

$$v(t) = \begin{cases} sin(2\pi f_1), & 0 \le t \le \frac{1}{f_1} \\ sin(2\pi f_2), & \frac{1}{f_1} < t \le \sum_{m=1}^{2}\frac{1}{f_m} \\ \quad \ldots & \quad \ldots \\ sin(2\pi f_M), & \sum_{m=1}^{M-1}\frac{1}{f_m} < t \le \sum_{m=1}^{M}\frac{1}{f_m} \end{cases} \tag{5}$$

where $1Hz \le f_m \le 95Hz$.

After continually iterative training, the final weights and thresholds which make the network error sum of squares minimum are determined. The hysteresis modeling result based on BPNN is shown in Fig. 4(a), the blue solid line and the red dotted line respectively represent the actual displacement and the output displacement of the modeling result. From the result, it can be seen that the hysteresis model describes the relationship between the input voltage and the output displacement with sufficiently high precision. And the output error between the actual out and the modeling output also demonstrates the modeling precision as the red dotted line shown in Fig. 4(b).

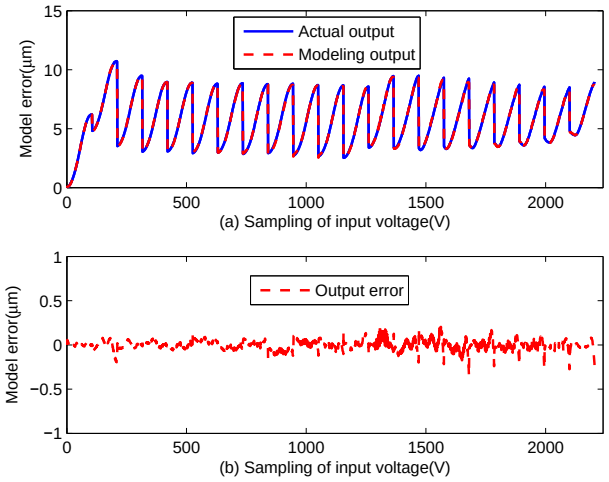

Fig. 4: The hysteresis modeling result

In order to show the modeling result more intuitively, we choose a set of sine voltage with frequency $5Hz$ as the input voltage to prove its performance. As shown in Fig. 5(a), the modeling output is basically the same with the actual output. And the model error of hysteresis loop in the forward and backward scanning process are respectively shown in Fig. 5(b)

and Fig. 5(c), which both demonstrate the high precision of the obtained hysteresis model based on the BPNN.

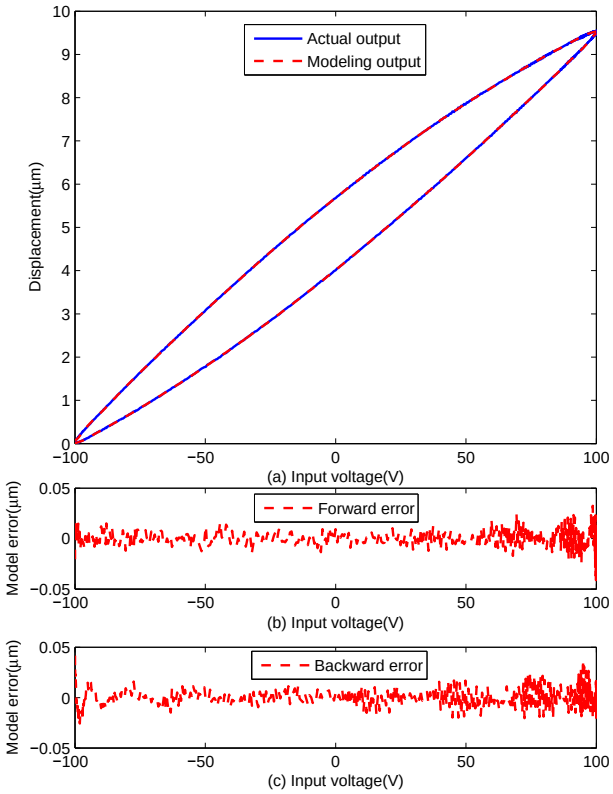

Fig. 5: The hysteresis modeling result with frequency $5Hz$

B. Compensation for the Hysteresis Behavior

After obtaining the hysteresis model, we propose a method based on cubic spline interpolation to compensate for the hysteresis behavior. In this section, we just take the forward scanning for example to introduce this method in detail, and the process of the backward scanning is compensated in the same way.

Because of the influence of the hysteresis nonlinearity, actually the coordinates of scanning points of each single row ($r_n = n, n \in \{1, 2, \dots N\}$) are not corresponding to the obtained height value of scanning ($\hat{H}_n, n \in \{1, 2, \dots N\}$), where N represents the number of scanning points of each single row. So as shown in Fig. 6, firstly, both the abscissa axis and ordinate axis of the hysteresis curve are evenly divided into N sections.

For each scanning point, we can get the voltage value v_n corresponding to the coordinate r_n as follows:

$$v_n = \frac{r_n}{k_v}$$

where k_v represents the slope of the input voltage and the desired displacement.

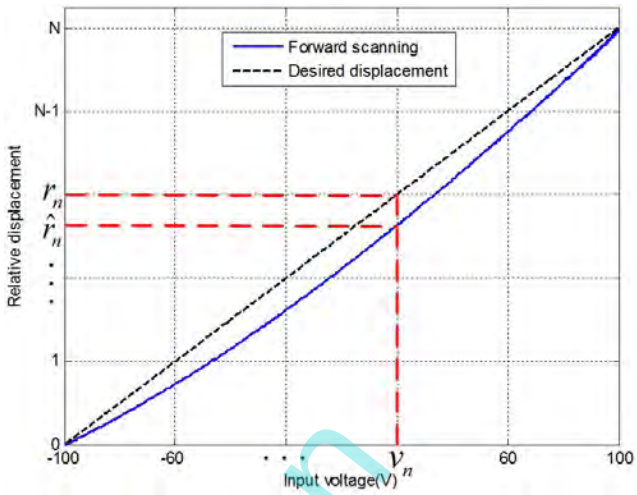

Fig. 6: The transformation of coordinates for the hysteresis compensation

Then the actual coordinates of the scanning points are calculated as follow:

$$\hat{r}_n = F(v_n, f)$$

where F represents the hysteresis model which can be obtained by the formula (1)-(4), f represents the frequency of the input voltage. Because $\hat{r}_n$ and $\hat{H}_n$ are truly matching, then we utilize cubic spline interpolation to calculate the height value H_n corresponding to r_n.

In cubic spline interpolation, a series of unique cubic polynomials are fitted between each of the data points, with the stipulation that the curve obtained be continuous and appear smooth [21]. These cubic splines can then be used to determine rates of change and cumulative change over an interval [22]. Based on this theory, H_n can be calculated as follows:

$$H_n = S(r_n), n \in \{1, 2, \dots N\}$$

where S is a piecewise function of the form

$$S(r_n) = \begin{cases} s_1(r_n), & \hat{r}_1 \le r_n \le \hat{r}_2 \\ s_2(r_n), & \hat{r}_2 < r_n \le \hat{r}_3 \\ \cdots & \cdots \\ s_3(r_n), & \hat{r}_{N-1} < r_n \le \hat{r}_N \end{cases} \tag{6}$$

where s_n is a third degree polynomial defined by

$$\begin{aligned} s_n(r_n) = a_n + b_n(r_n - \hat{r}_n) \\ + c_n(r_n - \hat{r}_n)^2 + d_n(r_n - \hat{r}_n)^3, \end{aligned} \tag{7}$$

and a_n, b_n, c_n, d_n are parameters which are determined by $\hat{r}_n$ and $\hat{h}_n$. By this method, the real height of the scanning points with the hysteresis compensation are obtained to image with high quality.

IV. Experiment Results

In the experiments, the proposed method is applied to the commercial Benyuan CSPM4000 AFM system to verify its performance. We use an optical grating sample with a feature height of $10nm$ to evaluate the AFM images [23]. The optical

grating is a kind of optical device which is composed of many parallel narrow gaps with fixed equal width and spacing [24]. Fig. 7 shows the standard image of the optical grating, which can be seen that the width of spacing in the image is fixed equal.

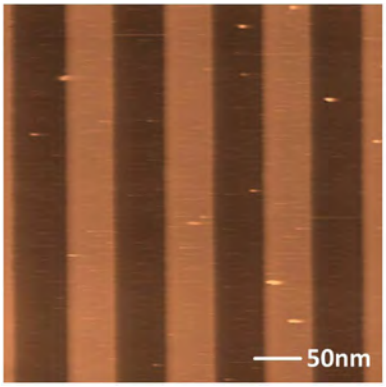

Fig. 7: The standard image of the optical grating

In the first experiment, the sample is scanned with frequency $5Hz$. As shown in Fig. 8, the blue solid line represents a row of the uncompensated scanning result of the optical grating. Because of the hysteresis nonlinearity, the left part of the blue solid line is much wider than the right part obviously, which is failed to reflect the real morphology of optical grating. After the compensation, the obtained height information is shown as the red dotted line, which has gaps with equal width and spacing and is more close to the real morphology of the optical grating.

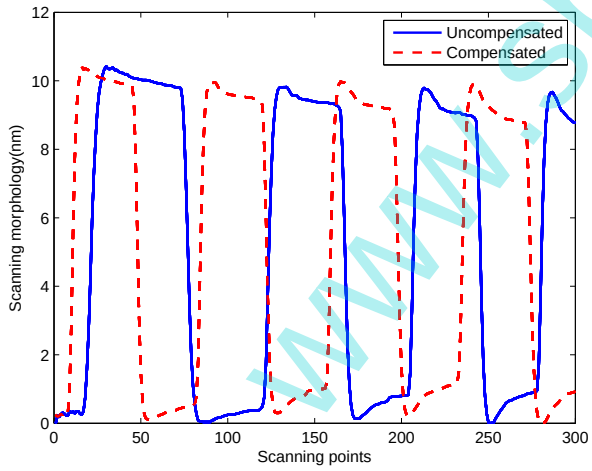

Fig. 8: A row of the uncompensated and compensated images with frequency $5Hz$

The scanning image of the optical grating in the first experiment is shown in Fig. 9, compared with the uncompensated scanning image of the optical grating, the compensated image reflects the real morphology more really.

Furthermore, in order to demonstrate the performance of our proposed method with high scanning frequency, in the

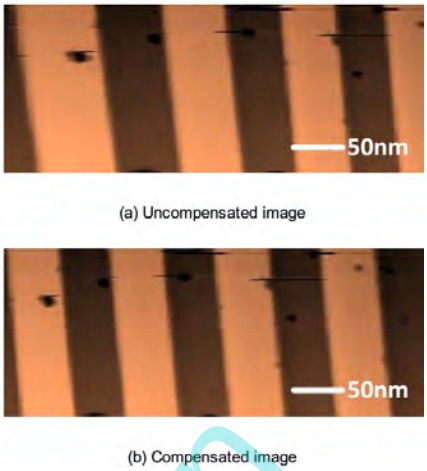

Fig. 9: The uncompensated and compensated images with frequency $5Hz$

second experiment, we apply this method to scan the sample with frequency $50Hz$. As shown in Fig. 10, the compensated image is more close to the real morphology of the optical grating than the uncompensated scanning image.

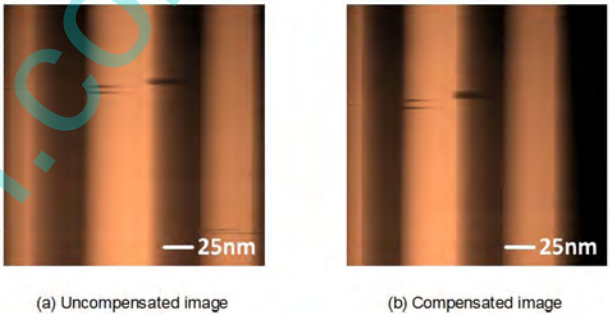

Fig. 10: The uncompensated and compensated images with frequency $50Hz$

V. Conclusion

In this paper, a two hidden layers BPNN consisting of an input layer, two hidden layers, and an output layer is utilized to model for the hysteresis effect of the piezoelectric scanner. Specifically, because of the memory characteristics and the frequency dependence of the hysteresis, both the frequency and a section of the input voltage are input to the BPNN. And the hysteresis modeling is obtained by constantly iterative training. Then we propose a method based on cubic spline interpolation to compensate for the hysteresis behavior effectively. The experiment results with low and high frequency both show that the proposed method improves the performance of the AFM system. In the future work, we will focus on the design of the BPNN in the hysteresis modeling and the research of the hysteresis compensation.

References

[1] A. Touhami, B. Nysten, and Y. F. Dufrene, Nanoscale mapping of the elasticity of microbial cells by atomic force microscopy, *Langmuir*, vol. 19, no. 11, pp. 4539-4543, 2003.

[2] Y. Huang, P. Cheng, and C. H. Menq, Dynamic force sensing using an optically trapped probing system, *IEEE/ASME Transactions on Mechatronics*, vol. 16, no. 6, pp. 1145-1154, 2011.

[3] M. A. Mabrok, A. G. Kallapur, I. R. Petersen, and A. Lanzon, Spectral conditions for negative imaginary systems with applications to nanopositioning, *IEEE/ASME Transactions on Mechatronics*, vol. 19, no. 3, pp. 895-903, 2014.

[4] F. J. Giessibl, Advances in atomic force microscopy, *Reviews of Modern Physics*, vol. 75, no. 3, pp. 949-983, 2003.

[5] M. Jobina, and R. Foschia, Versatile force-feedback manipulator for nanotechnology applications, *Review of Scientific Instruments*, vol. 76, no. 5, pp. 053701, 2005.

[6] M. N. Islam, and R. J. Seethaler, Sensorless position control for piezoelectric actuators using a hybrid position observer, *IEEE/ASME Transactions on Mechatronics*, vol. 19, no. 2, pp. 667-675, 2014.

[7] N. Hosseini, A. P. Nievergelt, J. D. Adams, V. T. Stavrov, and G. E. Fantner, A monolithic MEMS position sensor for closed-loop high-speed atomic force microscopy, *Nanotechnology*, vol. 27, no. 13, pp. 135705, 2016.

[8] Y. Cui, B. Sun, W. Dong, and Z. Yang, Causes for hysteresis and nonlinearity of piezoelectric ceramic actuators, *Optics and Precision Engineering*, vol. 11, no. 3, pp. 270-275, 2003.

[9] H. Tang, Y. Li, and X. Zhao, Hysteresis modeling and inverse feedforward control of an AFM piezoelectric scanner based on nano images, in *Proceedings of the 2011 IEEE International Conference on Mechatronics and Automation*, pp. 189-194, 2011.

[10] K. K. Leang, and S. Devasia, Feedback-linearized inverse feedforward for creep, hysteresis, and vibration compensation in AFM piezoactuators, *IEEE Transactions on Control Systems Technology*, vol. 15, no. 5, pp. 927-935, 2007.

[11] Y. Zhang, Y. Fang, X. Zhou, and X. Dong, Image-based hysteresis modeling and compensation for an AFM piezoscanner, *Asian Journal of Control*, vol. 11, no. 2, pp. 166-174, 2009.

[12] D. Habineza, M. Rakotondrabe, and Y. L. Gorrec, Bouc-wen modeling and feedforward control of multivariable hysteresis in piezoelectric systems: Application to a 3-DoF piezotube scanner, *IEEE Transactions on Control Systems Technology*, vol. 23, no. 5, pp. 1797-1806, 2015.

[13] A. T. C. Goh, Back-propagation neural networks for modeling complex systems, *Artificial Intelligence in Engineering*, vol. 9, no. 1, pp. 143-151, 1995.

[14] A. J. Fleming, and S. O. R. Moheimani, A grounded-load charge amplifier for reducing hysteresis in piezoelectric tube scanners, *Review of Scientific Instruments*, vol. 76, no. 7, pp. 073707, 2005.

[15] M. S. Rana, H. R. Pota, and I. R. Petersen, Nonlinearity effects reduction of an AFM piezoelectric tube scanner using MIMO MPC, *IEEE/ASME Transactions on Mechatronics*, vol. 20, no. 3, pp. 1458-1469, 2015.

[16] M. S. Rana, H. R. Pota, and I. R. Petersen, Performance of sinusoidal scanning with MPC in AFM imaging, *IEEE/ASME Transactions on Mechatronics*, vol. 20, no. 1, pp. 73-83, 2015.

[17] L. Wang, Y. Zeng, and T. Chen, Back propagation neural network with adaptive differential evolution algorithm for time series forecasting, *Expert Systems with Applications*, vol. 42, no. 2, pp. 855-863, 2015.

[18] S. Lee, and W. S. Choi, A multi-industry bankruptcy prediction model using back-propagation neural network and multivariate discriminant analysis, *Expert Systems with Applications*, vol. 40, no. 8, pp. 2941-2946, 2013.

[19] F. Chen, Back-propagation neural networks for nonlinear self-tuning adaptive control, *IEEE Control Systems Magazine*, vol. 10, no. 3, pp. 44-48, 1990.

[20] B. Mokaberi, and A. A. G. Requicha, Compensation of scanner creep and hysteresis for AFM nanomanipulation, *IEEE Transactions on Automation Science and Engineering*, vol. 5, no. 2, pp. 197-206, 2008.

[21] J. Huang, J. Tang, M. Zhang, X. Zhang, and T. Han, An improved EMD based on cubic spline interpolation of extremum centers, *Journal of Vibroengineering*, vol. 17, no. 5, pp. 2393-2409, 2015.

[22] W. Wu, T. Wang, and C. Chiu, Edge curve scaling and smoothing with cubic spline interpolation for image upscaling, *Journal of Signal Processing Systems*, vol. 78, no. 1, pp. 95-113, 2015.

[23] X. Zhou, Research on control of AFM based nano-imaging and nano-manipulation, *Ph. D Dissertation of Nankai University*, 2009.

[24] M. Prikockis, H. Wijesinghe, A. Chen, J. VanCourt, D. Roderick, and R. Sooryakumar, An on-chip colloidal magneto-optical grating , *Applied Physics Letters*, vol. 108, no. 16, pp. 161106, 2016.